Available online at www.sciencedirect.com
ScienceDirect
Trans. Nonferrous Met. Soc. China 24(2014) 1187−1195
Transactions of Nonferrous Metals Society of China
www.tnmsc.cn

Recovery of alumina from circulating fluidized bed combustion Al-rich fly ash using mild hydrochemical process

Quan-cheng YANG[1,2], Shu-hua MA[1], Shi-li ZHENG[1], Ran ZHANG[1]

1. Key Laboratory of Green Process and Engineering, Institute of Process Engineering, Chinese Academy of Sciences, Beijing 100190, China;
2. College of Environmental Engineering, North China Institute of Science and Technology, Beijing 101601, China

Received 8 April 2013; accepted 9 July 2013

Abstract: To utilize CFBC Al-rich fly ash, a mild hydrochemical extraction process was investigated for recovery of alumina. An alumina extraction efficiency of 92.31% was attained using a 45% NaOH solution, an original caustic ratio (molar ratio of Na_2O to Al_2O_3 in the sodium aluminate solution) of 25, a molar ratio of CaO to SiO_2 in the fly ash of 1.1, a liquid volume to solid mass ratio of 9, a reaction temperature of 280 °C, and a residence time of 1 h when treating fly ash with an alumina to silica mass ratio (A/S) of 0.78 and an alumina content of 32.43%. Additionally, the alumina leaching mechanism was explored via structural and chemical analysis, which revealed that after alkaline digestion, the main solid phase containing silica was $NaCaHSiO_4$ with a theoretical A/S of zero.

Key words: recovery of alumina; fly ash; phase transformation; circulating fluidized bed combustion (CFBC)

1 Introduction

Fly ash is a powdery residue generated mainly by coal-fired power plants. Since coal is still the major energy resource in China, the output of fly ash has increased continuously over the past several years, reaching 480 million tons in 2010 [1]. Presently, fly ash is consumed on a large scale in cement and concrete fillers as well as roadway and pavement utilization [2−5]. However, due to its rapid production, the fly ash is not completely consumed and is utilized at a rate of 66%−68%. There are huge quantities of fly ash stored in ash dams, making it the largest single source of solid waste in China and posing serious environmental and social problems [6,7]. Additionally, the current utilizations of fly ash primarily focus on low-value applications, such as the auxiliary construction materials mentioned above.

To achieve high-value utilization of fly ash, many studies on the extraction of alumina from fly ash have been performed using acid or base as the leaching agent [8−11]. In the 1950s, scientists from Poland explored a fly ash treatment using a limestone sintering process to recover the alumina [12]. In this scheme, fly ash was mixed with limestone and heated to 1300 °C, converting the alumina in the fly ash to calcium aluminate and the silica to dicalcium silicate. Based on the difference in solubility in sodium carbonate solution, calcium aluminate was separated from dicalcium silicate. However, this process is not compatible with large-scale industrialization due to high energy consumption and a large output of highly alkaline waste.

Several decades later, another process was successfully developed by a national laboratory in US using chloride acid to dissolve alumina in the fly ash, leaving the silica. However, mullite, the main type of fly ash generated by pulverized coal combustion (PCC) boilers, is stable under acidic conditions [9−13], necessitating a pre-sintering step in the acid leaching process to ensure complete mullite decomposition. Otherwise, only the amorphous alumina is leachable, limiting the total extraction ratio. Moreover, this kind of acidic process causes serious corrosion of the equipment, and impurities, such as iron, calcium, and titanium that were co-leached into the acid solution, are hard to

Foundation item: Project (2012BAF03B01) supported by the National Science and Technology Support Program of China; Project (2011AA060701) supported by the Hi-tech Research and Development Program of China
Corresponding author: Shu-hua MA; Tel: +86-13521118758; E-mail: shma@home.ipe.ac.cn
DOI: 10.1016/S1003-6326(14)63178-2

remove. Ultimately, acid leaching rarely produces high quality alumina but causes secondary pollution via the decomposition of aluminum chloride or sulfate.

Recently, a particular kind of fly ash has been found in Inner Mongolia and Shanxi Province, China. The mass content of alumina in the fly ash in these regions is over 30%, sometimes higher than 50%, with an annual output of about 50 million tons. It was found that apart from kaolinite, the major mineral component of conventional coal [14], the coal in these regions also contains boehmite as high as 7.2% (mineral matter basis) [12,15]. Accordingly, the fly ash generated from this coal is high in alumina, containing nearly the same amount as some forms of low-grade bauxite. Simultaneously, a cleaner and more advanced combustion technology, circulating fluidized bed combustion (CFBC), has become widely popular since 2004 in China[16]. The operating temperature of CFBC boilers is 800−950 °C, lower than that of conventional PCC, 1200−1400 °C[17]. The expansion of CFBC capacity has led to significant discharge rates of CFBC alumina-rich fly ash in the regions noted above. CFBC alumina-rich fly ash is characterized by amorphous alumina, irregular particle shape, and high sulfur and calcium contents.

1) Amorphous alumina. The amorphous phases in CFBC alumina-rich fly ash originate from the thermal decomposition of kaolinite and boehmite, and the former had been thoroughly characterized [18−20]. It is known that the amorphous phases are mainly amorphous silica and alumina formed by the decomposition of kaolinite at the combustion temperature. Additionally, boehmite decomposes at 800−950 °C into poor crystalline γ-Al_2O_3, which leads to a large quantity of amorphous alumina in CFBC alumina-rich fly ash.

2) Irregular particle shape. In general, CFBC alumina-rich fly ash significantly differs from that generated by PCC in terms of particle shape due to the different combustion temperatures. At 1200−1400 °C, the PCC boiler operational temperature range, some minerals enter a liquid state. When cooled, these minerals form spherical and semispherical grains with different sizes [21]. Conversely, the minerals in alumina-rich fly ash do not enter the liquid state at the lower temperature range used for CFBC, 800−950 °C, giving rise to irregular particle shapes.

3) Sulfur and calcium content. In the CFBC process, limestone is added to the boiler to absorb sulfur, which leads to relatively high sulfur and calcium contents in the fly ash. Because the limestone causes a dilution effect, the alumina content in CFBC alumina-rich fly ash, at 30%−40%, is not as high as that produced by PCC.

The output of CFBC alumina-rich fly ash has increased dramatically in recent years. The high alumina content makes it an attractive potential source of alumina, particularly for China because of its shortage of bauxite. Exploring new extraction processes for alumina from high-alumina fly ash is therefore of great significance.

Hydrochemical processes, first developed by a group of scientists from the former Soviet Union, can separate alumina from silica by generating $NaCaHSiO_4$, an insoluble alumina-free compound. This alkaline process has been successfully implemented for treating low-grade bauxite and nephelite [22,23]. The main focus of this study was to investigate the recovery of alumina from fly ash using the hydrochemical process and to elucidate the behavior of Al_2O_3 and SiO_2 during the reaction. Furthermore, the phase transformation of fly ash under alkali conditions was also examined.

2 Experimental

2.1 Raw materials and apparatus

Feed coal and CFBC Al-rich fly ash were obtained from a coal fired power plant in Shanxi Province, China. Samples of feed coal and fly ash were placed in an oven at 105 °C for 24 h. Representative samples were collected using the cone and quartering method.

All chemicals used, including sodium hydroxide and aluminum hydroxide, were of analytical grade and manufactured by China Xilong Chemical Co., Ltd. High-purity Milli-Q water, with a resistivity of below 18.2 MΩ·cm at ambient temperature, was used for all experiments.

A custom-made 500 mL stainless steel autoclave used to extract alumina from the fly ash was equipped with a mechanical agitator, a temperature control system with a precision of 0.2 °C, and a water cooling system. To protect the autoclave from corrosion from the high alkaline solution, it was lined with pure nickel.

Inductively coupled plasma optical emission spectrometer (ICP-OES, PE Optima 5300DV, Perkin-Elmer) was used to analyze the liquid and solid chemical composition of the samples. The phase of the equilibrium solid was identified by X-ray diffraction (XRD, Philips PW226/30 with Cu K_α radiation, 40 kV, and 100 mA). Morphology and mineralogical analyses were conducted using scanning electron microscope (SEM, JEOL 5800SV). Particle size distribution analyses were carried out using a Mastersizer 2000 (Malvern).

2.2 Experimental methods

To extract alumina from the fly ash, experiments were carried out in the 500 mL stainless steel autoclave. Each experiment was performed by mixing 25 g of fly

ash with a predetermined volume of sodium aluminate solution with a high caustic ratio and high molar ratio of calcium oxide. The mixture was stirred at constant speed and heated to the desired reaction temperature. Once the reaction completed, the products were quickly cooled to 90 °C using cold water. The factors influencing the extraction rate of alumina from the fly ash, including the sodium hydroxide solution concentration, reaction temperature, liquid volume to solid mass ratio (L/S), and molar ratio of CaO to SiO_2 (C/S, controlled through the amount of CaO added), were assessed independently. After the reaction, the slurry was filtered to obtain a solution and a solid residue. The residue was washed twice with deionized water at 80 °C then dried in an oven at 105 °C for 12 h. The dried sample was ground into a powder for characterization.

3 Results and discussion

3.1 Characterization of raw materials

The results of the feed coal phase analysis are shown in Fig. 1. The mineral phases identified were quartz (SiO_2), kaolinite ($Al_2O_3·2SiO_2·2H_2O$), pyrite (FeS_2), and calcite ($CaCO_3$). Phase analysis results also revealed that the feed coal contained relatively high amounts of kaolinite, which may be the largest contributor to the high alumina content in fly ash. Its loss on ignition was found to be 77.42%.

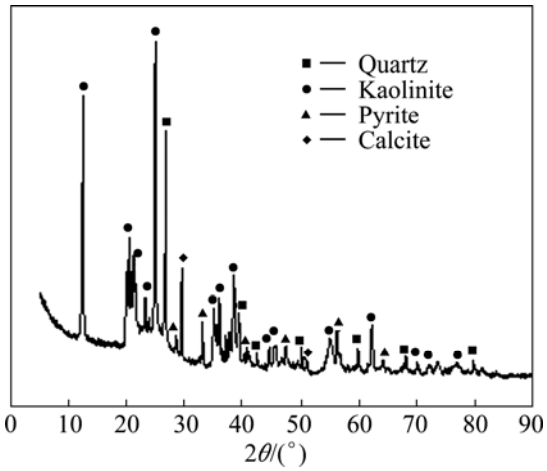

Fig. 1 XRD pattern of unburned coal

The results of the chemical analysis of the fly ash are shown in Table 1. They revealed that Al_2O_3, SiO_2, Fe_2O_3, CaO, and TiO_2 were the principle components of the fly ash, and that the mass ratio of alumina to silica (A/S) was 0.78, slightly lower than the theoretical value for kaolinite due to the presence of quartz. The contents of Al_2O_3 and SiO_2, the two key components, were found to be 32.43% and 41.77%, respectively, with a combined content of nearly 75%. Figure 2 shows the particle size distribution (from 0.3 to 500 μm) of the fly ash, with a volume average particle diameter of 42.91 μm. The mineralogy phases of the fly ash were also examined, as shown in Fig. 3. The identified crystalline phases included quartz (SiO_2), magnetite (Fe_3O_4), portlandite ($Ca(OH)_2$), gypsum ($CaSO_4·2H_2O$), and ettringite ($Ca_6Al_{l2}(SO_4)_3(OH)_{12}32H_2O$). The broad diffraction peaks at 20°−30° in the XRD pattern indicated the presence of considerable amorphous matter in the fly ash. No alumina-bearing crystalline phase was observed in the sample, indicating that Al in the fly ash was dominant in the amorphous glass phase. SEM images of the fly ash are shown in Fig. 4, revealing a smooth surface and irregular shapes.

Table 1 Chemical composition of fly ash

$w(Al_2O_3)$/ %	$w(SiO_2)$/ %	$w(Fe_2O_3)$/ %	$w(CaO)$/ %	$w(TiO_2)$/ %	$w(Na_2O)$/ %	A/S
32.43	41.77	3.18	9.41	1.12	0.17	0.78

A/S: mass ratio of Al_2O_3 to SiO_2

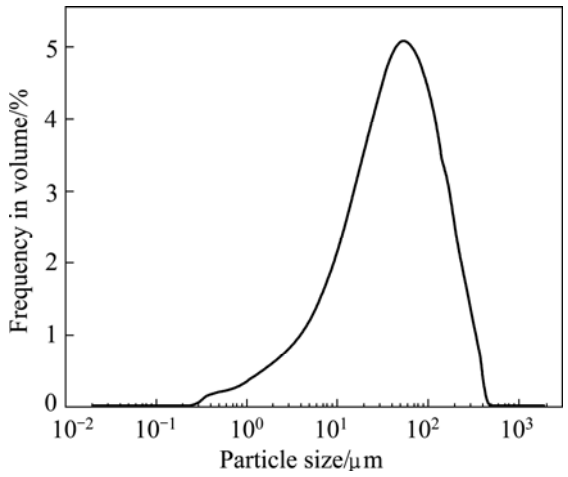

Fig. 2 Particle size distribution of fly ash

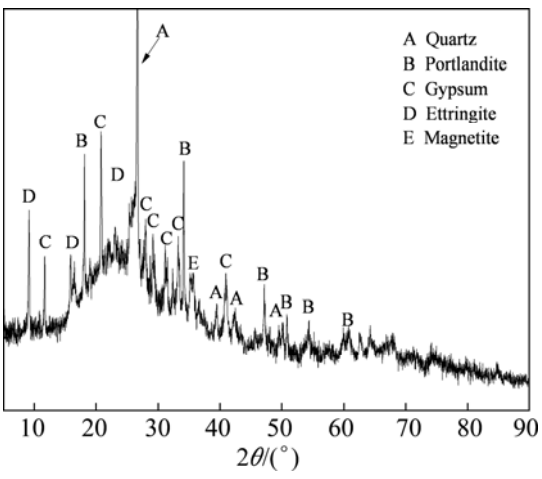

Fig. 3 XRD pattern of fly ash

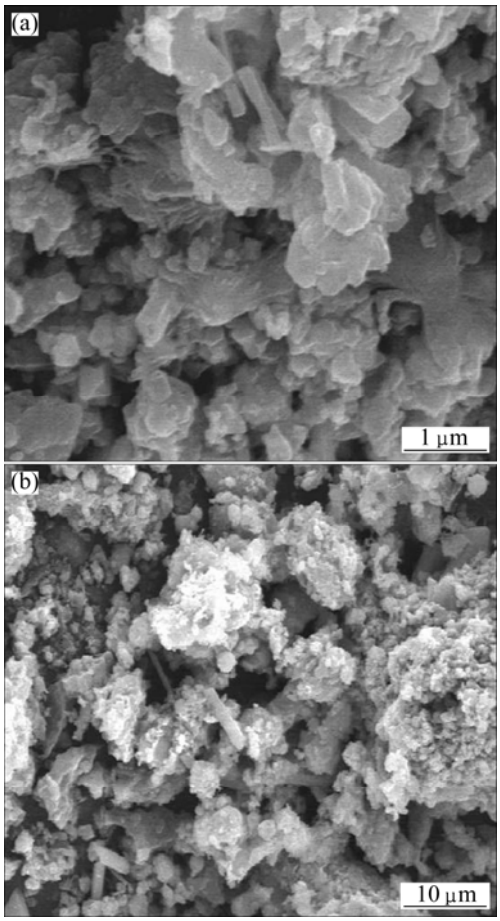

Fig. 4 SEM images of fly ash

3.2 Factors affecting extraction rate of alumina from fly ash

3.2.1 Effect of NaOH concentration

To determine the effect of NaOH concentration on the extraction rate of alumina, experiments were performed using an initial caustic ratio of 25, reaction temperature of 280 °C, C/S of 1:1, L/S of 9, and residence time of 2 h. NaOH concentrations 35%−60% were tested. The results are shown in Table 2, Figs. 5 and 6.

Table 2 shows that Na_2O content of the leached residue first increased and then decreased with the growing of NaOH concentration, and it reached a maximum at NaOH concentration of 45%. As the leached residue contains a relatively high content of Na_2O, it needs subsequent treatment to recover Na_2O.

From Fig. 5, it is clear that the extraction rate of Al_2O_3 from fly ash increased sharply as the NaOH concentration increased from 35% to 45%, then decreased when the NaOH concentration exceeded 45%. Conversely, the A/S of the leaching residue decreased in 35%−45% NaOH, and then increased at higher NaOH concentrations.

Figure 6 shows the XRD patterns for samples with NaOH concentrations of 35%, 45%, and 55%. At a

Table 2 Na_2O content of leached residue at various NaOH concentrations in mass fraction

NaOH concentration/%	35	40	45	50	55	60
Na_2O content/%	13.92	17.36	19.13	17.97	17.85	17.45

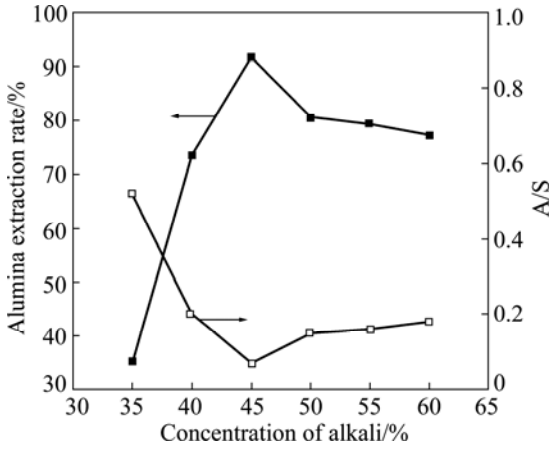

Fig. 5 Effect of NaOH concentration on alumina extraction rate and A/S of leaching residue (reaction temperature of 280 °C, C/S of 1:1, L/S of 9, and residence time of 2 h)

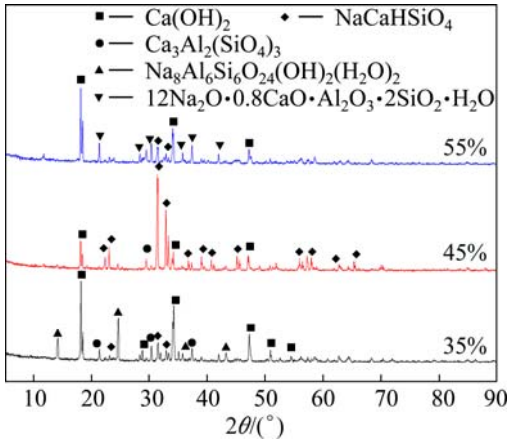

Fig. 6 XRD patterns of residues obtained under different alkali concentrations

NaOH concentration of 35%, the crystal phases were mainly $Na_8Al_6Si_6O_{24}(OH)_2(H_2O)_2$, $Ca_3Al_2(SiO_4)_3$, and $Ca(OH)_2$, as well as $NaCaHSiO_4$, which exhibited weak peaks. The presence of $Na_8Al_6Si_6O_{24}(OH)_2(H_2O)_2$ and $Ca_3Al_2(SiO_4)_3$ led to a low alumina extraction rate and a high A/S of the leaching residue. At a NaOH concentration of 45%, the $Na_8Al_6Si_6O_{24}(OH)_2(H_2O)_2$ peaks completely disappeared and strong $NaCaHSiO_4$ peaks emerged, indicating that a high alumina extraction rate was obtained. As the concentration of NaOH continued to increase, the $NaCaHSiO_4$ peaks weakened and $1.2Na_2O{\cdot}0.8CaO{\cdot}Al_2O_3{\cdot}2SiO_2{\cdot}H_2O$ peaks emerged, which provides an explanation for the lower alumina extraction rate at NaOH concentrations >45%. The

results of XRD analyses further prove high content of Na_2O in leached residue mainly due to the presence of sodium-containing phase $Na_8Al_6Si_6O_{24}(OH)_2(H_2O)_2$, $NaCaHSiO_4$ and $1.2Na_2O{\cdot}0.8CaO{\cdot}Al_2O_3{\cdot}2SiO_2{\cdot}H_2O$. Phase analyses make it clear that the variations of A/S and Na_2O content are essentially caused by crystal phase transformation, and when the phase of $NaCaHSiO_4$ becomes dominant, the contents of Na_2O and Al_2O_3 reach their extreme values respectively.

3.2.2 Effect of L/S

The experiments investigating the effect of the L/S were carried out at a caustic ratio of 25, a temperature of 280 °C, a C/S of 1:1, a NaOH concentration of 45%, and a residence time of 2 h. The L/S was varied within the range of 7−13. Figures 7 and 8 show the fluctuation in the alumina extraction rate and the A/S of the leaching residue as the L/S increased.

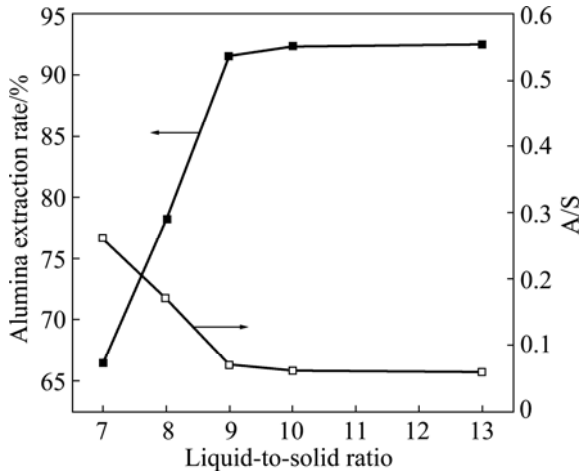

Fig. 7 Effect of L/S on alumina extraction rate and A/S of leaching residue (reaction temperature of 280 °C, C/S of 1:1, NaOH concentration of 45%, and residence time of 2 h)

As shown in Fig. 7, the extraction rate of Al_2O_3 increased linearly with increasing L/S while the A/S of the leaching residue decreased, revealing an inverse relationship between these parameters. However, when the L/S was higher than 9, the extraction rates were relatively constant. Hence, an L/S of 9 was selected as the optimal value.

Figure 8 shows the XRD patterns of residues after leaching at various L/S values. At a L/S of 7, the crystal phases were mainly $NaCaHSiO_4$ and $Ca_3Al_2(SiO_4)_3$; as the ratio increased, however, the $Ca_3Al_2(SiO_4)_3$ peaks weakened and the $NaCaHSiO_4$ peaks enhanced. The changes in crystal phase explain the increased alumina extraction rate well with the increase in L/S.

3.2.3 Effect of reaction temperature

To study the effect of reaction temperature, experiments were performed using a NaOH concentration of 45%, C/S of 1:1, caustic ratio of 25, L/S of 9, and residence time of 2 h. The temperature was tested within the range of 230−300 °C. The results are shown in Figs. 9 and 10.

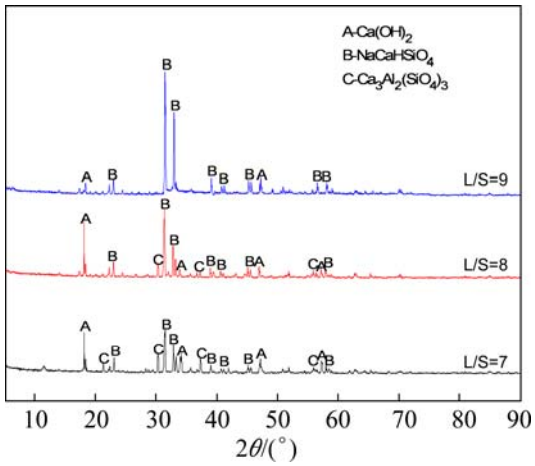

Fig. 8 XRD patterns of residues obtained at different L/S values

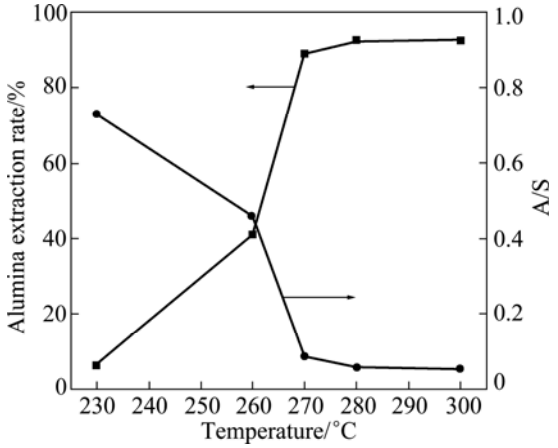

Fig. 9 Effect of digestion temperature on alumina extraction rate and A/S of leaching residue (NaOH concentration of 45%, L/S of 9, C/S of 1:1, and residence time of 2 h)

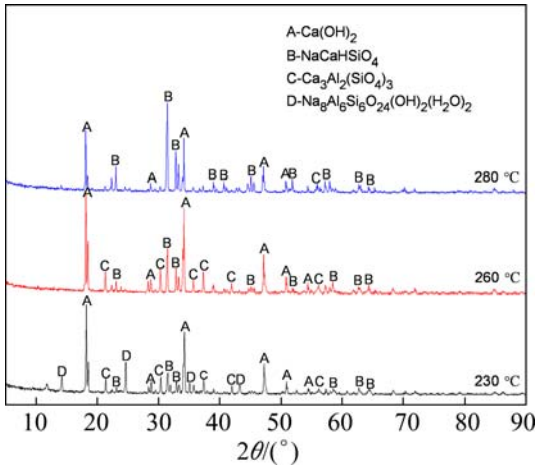

Fig. 10 XRD patterns of residues after leaching at different temperatures

As seen in Fig. 9, the extraction rate of Al_2O_3 increased with increasing reaction temperature from 230 °C to 300 °C and the A/S of the leaching residue decreased, with high temperature significantly improving the extraction of alumina. Figure 10 shows the phase transformations that occurred with increasing temperature. The trends in the extraction rate of Al_2O_3 and the A/S of the leaching residue are indicated by the XRD patterns, revealing that the low level of alumina extraction and high A/S of the leaching residue were due to the presence of $Na_8Al_6Si_6O_{24}(OH)_2(H_2O)_2$ and $Ca_3Al_2(SiO_4)_3$ at relatively low temperatures. The $Na_8Al_6Si_6O_{24}(OH)_2(H_2O)_2$ peaks disappeared and transformed into $NaCaHSiO_4$ and $Ca_3Al_2(SiO_4)_3$ peaks when the reaction temperature reached 260 °C. As the temperature continued to increase, the $Ca_3Al_2(SiO_4)_3$ peaks weakened while those of $NaCaHSiO_4$ enhanced. When the temperature reached 280 °C, the main phase of the residue turned almost completely to $NaCaHSiO_4$, and the alumina in the fly ash was largely extracted.

3.2.4 Effect of C/S

The experiments elucidating the effects of varying the C/S ratios were conducted at a caustic ratio of 25, a temperature of 280 °C, an L/S of 9, a NaOH concentration of 45%, and a residence time of 2 h at various C/S values. Figures 11 and 12 show the trends in the alumina extraction rate and the A/S of the leaching residue as the C/S increased, which was accomplished by varying the amount of CaO added to the reaction mixture.

Figure 12 shows the XRD patterns for samples with C/S values ranging from 0.9 to 1.3. At C/S values of 0.9 and 1.0, the crystal phases detected were mainly $Ca(OH)_2$, $NaCaHSiO_4$, and $Na_8Al_6Si_6O_{24}(OH)_2(H_2O)_2$. As the ratio approached 1.1, the $Na_8Al_6Si_6O_{24}(OH)_2(H_2O)_2$ peaks disappeared while the principal phase converted to $Ca(OH)_2$ and $NaCaHSiO_4$. At C/S of 1.2, a $Ca_3Al_2(SiO_4)_3$ phase formed. These results indicate that establishing an improper C/S leads to low alumina extraction efficiency due to the formation of an alumina-bearing phase ($Na_8Al_6Si_6O_{24}(OH)_2(H_2O)_2$ and $Ca_3Al_2(SiO_4)_3$.)

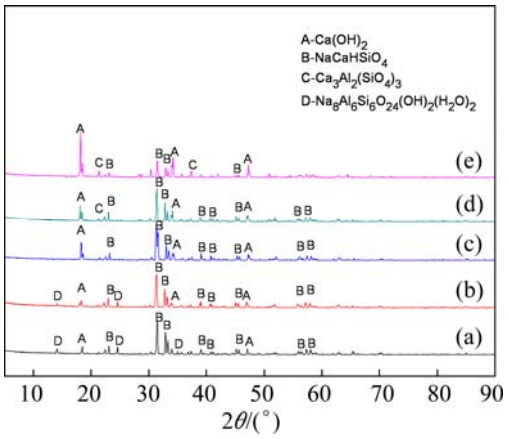

Fig. 12 XRD patterns of residues obtained with different C/S values: (a) C/S=0.9; (b) C/S=1.0; (c) C/S=1.1; (d) C/S=1.2; (e) C/S=1.3

3.2.5 Impact of residence time

Residence time is not only an important process parameter in extracting alumina from fly ash, but is also an important consideration in designing leaching reactors. Experiments elucidating the effects of varying residence times were performed at a caustic ratio of 25, a reaction temperature of 280 °C, an L/S of 9, a NaOH concentration of 45%, and a C/S of 1.1:1. The residence time was varied from 30 min to 120 min. The results are shown in Fig. 13.

From Fig. 13, it is clear that the extraction rate of

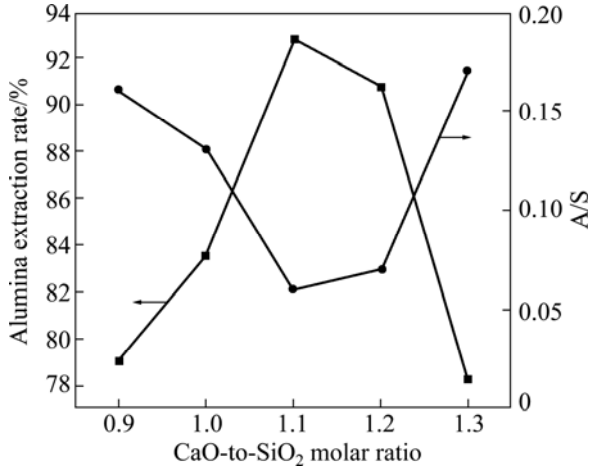

Fig. 11 Effects of C/S on alumina extraction rate and A/S of leaching residue (reaction temperature of 280 °C, NaOH concentration of 45%, L/S of 9, and residence time of 2 h)

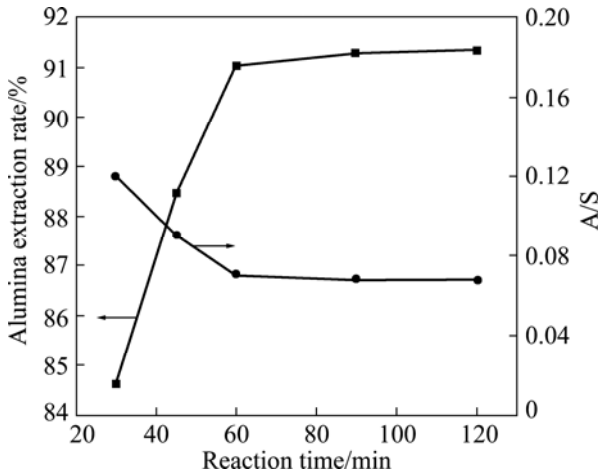

Fig. 13 Effects of digestion time on alumina extraction rate and A/S of leaching residue (reaction temperature of 280 °C, NaOH concentration of 45%, L/S of 9, and C/S of 1.1)

Al_2O_3 increased rapidly as residence time increased from 30 to 60 min, while the A/S of the leaching residue decreased. However, when the residence time exceeded 60 min, the extraction ratios stabilized. Therefore, the optimal residence time for extracting alumina was identified as 60 min.

3.2.6 Optimum conditions

From the experiments described above, we determined the optimum conditions for recovering alumina from fly ash generated by a circulating fluidized bed boiler as follows: NaOH concentration 45%, C/S 1.1:1, L/S 9, temperature 280 °C, and residence time 60 min. Under these conditions, the extraction rate of alumina was as high as 92.31%.

3.3 Characteristics of leached residue

The XRD patterns of leached residue under optimum conditions are shown in Fig. 14, indicating that the main phase of the leached residue was $NaCaHSiO_4$ with a theoretical A/S at the ideal value of zero. Phase analysis confirmed that the separation of Al and Si in fly ash was accomplished via hydrochemical treatment, and that the alumina in the fly ash was extracted efficiently through the formation of $NaCaHSiO_4$.

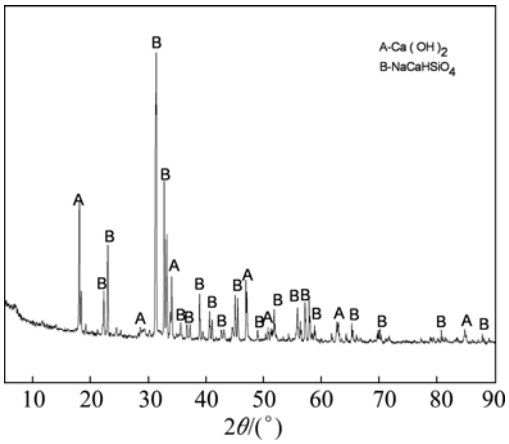

Fig. 14 XRD pattern of fly ash residue obtained under optimum conditions

The composition of the leached residue using the optimum conditions is listed in Table 3. Compared with the corresponding values in raw fly ash, the Al_2O_3 content and A/S in the leached residue decreased significantly after the leaching process, falling to 1.89% and 0.06, respectively. Meanwhile, the calcium and sodium contents increased significantly compared with untreated fly ash due to the formation of the $NaCaHSiO_4$ dominant phase. So, in order to realize circulation of alkaline liquor, recovery of sodium from leached residue becomes an important step.

Table 3 Composition of leached residue obtained under optimum conditions

$w(Al_2O_3)$/ %	$w(SiO_2)$/ %	$w(Fe_2O_3)$/ %	$w(CaO)$/ %	$w(TiO_2)$/ %	$w(Na_2O)$/ %	A/S
1.89	30.67	1.03	34.91	0.86	19.22	0.06

3.4 Recovery of sodium oxide

As the main phase of leached residue is $NaCaHSiO_4$, the decomposition of $NacaHSiO_4$ is the key step for recovery of sodium from leached residue. Previous studies have demonstrated that $NaCaHSiO_4$ can be broken down easily in dilute alkali solution [24]. The experiment results also demonstrates that the Na_2O content of the final residue can reduce to 0.86%, as shown in Table 4, under conditions of Na_2O concentration of 30 g/L, temperature of 170 °C. Figure 15 shows that the phase of the final residue transformed into $Ca_5(OH)_2Si_6O_{16}·4H_2O$ (tobermorite), which theoretically contains no sodium oxide.

Table 4 Composition of final residue after sequential extractions of alumina and sodium oxide

$w(Al_2O_3)$/ %	$w(SiO_2)$/ %	$w(Fe_2O_3)$/ %	$w(CaO)$/ %	$w(TiO_2)$/ %	$w(Na_2O)$/ %
2.89	32.77	1.64	35.91	1.00	0.86

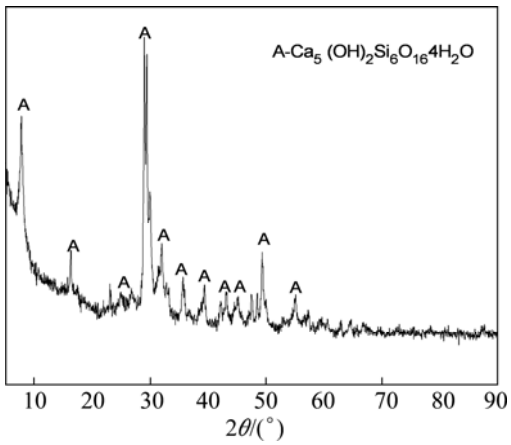

Fig. 15 XRD pattern of final residue after sequential extractions of alumina and sodium oxide

4 Alumina leaching mechanism

4.1 Temperature-dependence of phase transformation

In order to explore the temperature dependence of phase transformation, experiments were conducted with a caustic ratio of the initial sodium aluminate solution of 25, an L/S of 9, a NaOH concentration of 45%, and a C/S of 1.1:1. The mixture was heated from 120 °C to the desired temperature. During the heating program, the reaction slurry was sampled at 170, 200, 230, 260, and 280°C, and the heating power of the autoclave was kept at a constant value.

The XRD patterns of leached residues at different reaction temperatures are shown in Fig. 16. Once the reaction temperature reached 170 °C, the phases of the leached residue had clearly transformed. The main characteristic peaks present in the XRD patterns of the fly ash disappeared, and characteristic peaks of $Na_8(Al_6Si_6O_{24})(OH)_2(H_2O)_2$ emerged. At 200 °C, the $Na_8(Al_6Si_6O_{24})(OH)_2(H_2O)_2$ peaks were still present, but weak peaks indicating the presence of $Ca_3Al_2(SiO_4)_3$ emerged. At 230 °C, the peak intensities of $Na_8(Al_6Si_6O_{24})(OH)_2(H_2O)_2$ and $Ca_3Al_2(SiO_4)_3$ increased, and new peaks indicating the presence of $NaCaHSiO_4$ appeared at 31.35°. At 260 °C, the peak intensities of $Na_8(Al_6Si_6O_{24})(OH)_2(H_2O)_2$ and $Ca_3Al_2(SiO_4)_3$ began to decrease and those of $NaCaHSiO_4$ began to increase. At 280 °C, the $Na_8(Al_6Si_6O_{24})(OH)_2(H_2O)_2$ and $Ca_3Al_2(SiO_4)_3$ peaks had nearly completely disappeared and the $NaCaHSiO_4$ peaks were significantly stronger. Thus, increasing the temperature from 120 °C to 280 °C caused the fly ash to experience a series of phase transformations, ultimately into $NaCaHSiO_4$. The production of $NaCaHSiO_4$, which contains no alumina, enables the efficient extraction of alumina from fly ash.

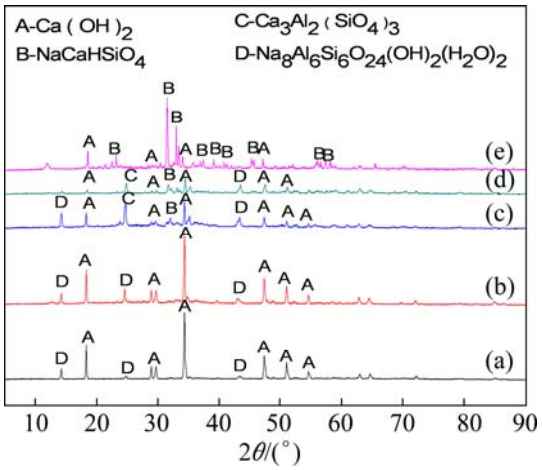

Fig. 16 XRD patterns of fly ash residues obtained at different temperatures: (a) 170 °C; (b) 200 °C; (c) 230 °C; (d) 260 °C; (e) 280 °C

4.2 Analysis of reaction principle

It is well known that the reaction principle of extracting alumina from bauxite by the Bayer method is based on chemical reaction equations (1) and (2). SiO_2 in bauxite can be converted into a sodium alumino−silicate hydrate precipitate, while Al_2O_3 in bauxite can be converted into soluble sodium aluminate. Thus, the separation of Al and Si in bauxite can be realized. However, constrained by the equilibrium solid phase of the leached residue, the Bayer method is applicable only to high grade bauxite. Fly ash, as a lower grade aluminum-containing resource with A/S ratios ranging from 0.7 to 1.0, is not compatible by the Bayer method.

$$Al_2O_3+2NaOH+3H_2O\rightarrow 2NaAl(OH)_4 \quad (1)$$

$$2SiO_2+2NaAl(OH)_4\rightarrow Na_2O\cdot Al_2O_3\cdot 2SiO_2\cdot nH_2O+(4-n)H_2O \quad (2)$$

Considering the hydrochemical process, we conclude from our experimental results that the principles of alumina extraction from fly ash are quite different from those concerning bauxite. Al_2O_3 in fly ash may be converted into sodalite/grossularite and soluble sodium aluminate depending on reaction conditions, while SiO_2 can be converted into sodalite/grossularite and insoluble $NaCaHSiO_4$. In order to extract alumina from fly ash, the desired phase is $NaCaHSiO_4$, which is created through reaction equation (3) under the optimum conditions. However, undesired phases consisting predominantly of sodalite and grossularite can emerge via reaction equations (4) and (5) under some conditions, such as low alkaline concentration, L/S, reaction temperature, C/S, and residence time.

$$SiO_2+NaOH+Ca(OH)_2\rightarrow H_2O+NaCaHSiO_4 \quad (3)$$

$$8NaOH+6SiO_2+3Al_2O_3+H_2O\rightarrow Na_8Al_6Si_6O_{24}(OH)_2(H_2O)_2 \quad (4)$$

$$6SiO_2+3Al_2O_3+Ca(OH)_2\rightarrow 3H_2O+Ca_3Al_2(SiO_4)_3 \quad (5)$$

For the reasons explained above, the hydrochemical process is useful for realizing efficient alumina extraction from fly ash through a range of phase transformations.

5 Conclusions

The process of leaching alumina from fly ash via the hydrothermal process was investigated in detail. The results showed that the highly effective decomposition of fly ash was obtained using this process, meaning that it has excellent potential for large-scale applications. Factors influencing the alumina extraction from the fly ash were explored, including the reaction temperature, NaOH concentration, L/S, residence time, and C/S. The optimum conditions were identified as: NaOH concentration, 45%; temperature, 280 °C; C/S, 1.1; L/S 9; and residence time, 1 h. Under these conditions, the A/S of the leaching residue and the alumina extraction rate were found to be 0.06 and 92.31%, respectively. By recovering Na_2O, the Na_2O content of the final residue can be controlled within 1.0% and total alkali consumption of the process is obviously less than that of Bayer process. The mechanism of alumina extraction from fly ash was also studied, which contributes to the formation of $NaCaHSiO_4$ with a theoretical A/S of zero, for materials containing alumina and silica.

References

[1] Ministry of industry and information technology. The 12th Five-Year Plan for Utilization of the Industrial Solid Wastes, 2012.

[2] CHINDAPRASIRT P, JATURAPITAKKUL C, SINSIRI T. Effect of fly ash fineness on microstructure of blended cement paste [J]. Construction and Building Materials, 2007, 21: 1534−1541.

[3] CHINDAPRASIRT P, RATTANASAK U. Utilization of blended fluidized bed combustion (FBC) ash and pulverized coal combustion (PCC) fly ash in geopolymer [J]. Waste Management, 2010, 30: 667−672.

[4] XU Hui, LI Qin, SHEN Li-feng, WANG Wei, ZHAI Jian-ping. Synthesis of thermostable geopolymer from circulating fluidized bed combustion (CFBC) bottom ashes [J]. Journal of Hazardous Materials, 2010, 175: 198−204.

[5] ABERG A, KUMPIENE J, ECKE H. Evaluation and prediction of emissions from a road built with bottom ash from municipal solid waste incineration (MSWI) [J]. Science of the Total Environment, 2006, 355: 1−12.

[6] FINKELMAN R B, OREM W, CASTRANOVA V, TATU C A, BELKIN H E, ZHENG B, LERCH H E, MAHARAJ S V, BATES A L. Health impacts of coal and coal use: Possible solutions [J]. International Journal of Coal Geology, 2002, 50: 425−443.

[7] HUGGINS F, GOODARZI F. Environmental assessment of elements and polyaromatic hydrocarbons emitted from a Canadian coal-fired power plant [J]. International Journal of Coal Geology, 2009, 77: 282−288.

[8] CAO D Z, SELIC, E, HERBELL J D. Utilization of fly ash from coal-fired power plants in China [J]. Journal of Zhejiang University: Science A, 2008, 9(5): 681−687.

[9] MATJIE R, BUNT J, VAN HEERDEN J. Extraction of alumina from coal fly ash generated from a selected low rank bituminous South African coal [J]. Minerals Engineering, 2005, 18: 299−310.

[10] NAYAK N, PANDA C R. Aluminium extraction and leaching characteristics of Talcher Thermal Power Station fly ash with sulphuric acid [J]. Fuel, 2010, 89: 53−58.

[11] QUEROL X, UMANA J, ALASTUEY A, AYORA C, LOPEZ-SOLER A, PLANA F. Extraction of soluble major and trace elements from fly ash in open and closed leaching systems [J]. Fuel, 2001, 80: 801−813.

[12] ZHANG Zhan-jun. Research on extraction of alumina and other useful resources from high aluminium fly ash [D]. Xi'an: Northwest University, 2007. (in Chinese)

[13] CHEN-TAN N W, van RIESSEN A, LY C V, SOUTHAM D C. Determining the reactivity of a fly ash for production of geopolymer [J]. Journal of the American Ceramic Society, 2009, 92: 881−887.

[14] DEMIR I, HUGHES R E, DEMARIS P J. Formation and use of coal combustion residues from three types of power plants burning Illinois coals [J]. Fuel, 2001, 80: 1659−1673.

[15] DAI Shi-feng, LI Dan, CHOU Chen-lin, ZHAO Lei, ZHANG Yong, REN De-yi, MA Yu-wen, SUN Ying-ying. Mineralogy and geochemistry of boehmite-rich coals: New insights from the Haerwusu Surface Mine, Jungar Coalfield, Inner Mongolia, China [J]. International Journal of Coal Geology, 2008, 74: 185−202.

[16] XIAO Xian-bin, YANG Hai-rui, ZHANG Hai, LU Jun-fu, YUE Guang-xi. Research on carbon content in fly ash from circulating fluidized bed boilers [J]. Energy & Fuels, 2005, 19: 1520−1525.

[17] XU Hui, LI Qin, SHEN Li-feng, ZHANG Meng-qu, ZHAI Jian-ping. Low-reactive circulating fluidized bed combustion (CFBC) fly ashes as source material for geopolymer synthesis [J]. Waste Management, 2010, 30: 57−62.

[18] CHAKRABORTY A K. DTA study of preheated kaolinite in the mullite formation region [J]. Thermochimica Acta, 2003, 398: 203−209.

[19] SANZ J, MADANI A, SERRATOSA J, MOYA J, AZA S. Aluminum-27 and silicon-29 magic-angle spinning nuclear magnetic resonance study of the kaolinite-mullite transformation [J]. Journal of the American Ceramic Society, 2005, 71: C418−C421.

[20] WHITE S, CASE E. Characterization of fly ash from coal-fired power plants [J]. Journal of Materials Science, 1990, 25: 5215−5219.

[21] CHINDAPRASIRT P, RATTANASAK U, JATURAPITAKKUL C. Utilization of fly ash blends from pulverized coal and fluidized bed combustions in geopolymeric materials [J]. Cement and Concrete Composites, 2011, 33: 55−60.

[22] ZHONG Li, ZHANG Yi-fei, ZHANG Yi. Extraction of alumina and sodium oxide from red mud by a mild hydro-chemical process [J]. Journal of Hazardous Materials, 2009, 172: 1629−1634.

[23] BI Shi-wen. Alumina production process [M]. Beijing: Chemical Industry Press, 2006. (in Chinese)

[24] ZHANG Ran, MA Shu-hua, YANG Quan-cheng, ZHENG Shi-li. Research on $NaCaHSiO_4$ decomposition in sodium hydroxide solution [J]. Hydrometallurgy, 2011, 108: 205−213.

温和水热法从循环流化床粉煤灰中回收氧化铝

杨权成[1,2]，马淑花[1]，郑诗礼[1]，张 然[1]

1. 中国科学院 过程工程研究所 绿色过程与工程重点实验室，北京 100190；
2. 华北科技学院 环境工程学院，北京 101601

摘 要：开发一种温和水热法从电厂排放的粉煤灰中提取氧化铝。当处理氧化铝和二氧化硅的质量比(A/S)为 0.78、氧化铝含量为 32.43%的粉煤灰时，在 NaOH 浓度 45%、初始苛性比(铝酸钠溶液中氧化钠和氧化铝的摩尔比)25、氧化钙和粉煤灰中二氧化硅的摩尔比 1.1、液固体积质量比 9、反应温度 280 °C、停留时间 1 h 的条件下，氧化铝的提取率可达到 92.31%。此外，通过结构和化学分析，对氧化铝的浸出机理进行了研究。结果表明，经过碱浸后，含硅的主要物相为理论铝硅比为 0 的 $NaCaHSiO_4$。

关键词：回收氧化铝；粉煤灰；物相变化；循环流化床

(Edited by Hua YANG)